Radiology

ORIGINAL RESEARCH • NEURORADIOLOGY

Focused Ultrasound–mediated Liquid Biopsy in a Tauopathy Mouse Model

Christopher Pham Pacia, PhD • Jinyun Yuan, PhD • Yimei Yue, BSc • Eric C. Leuthardt, MD • Tammie L. S. Benzinger, MD, PhD • Arash Nazeri, MD • Hong Chen, PhD**

From the Department of Biomedical Engineering, Washington University in St Louis, 4511 Forest Park Ave, St Louis, MO 63108 (C.P.P., J.Y., Y.Y., E.C.L., H.C.); Department of Neurosurgery (E.C.L.), Mallinckrodt Institute of Radiology (T.L.S.B., A.N.), and Department of Radiation Oncology (H.C.), Washington University School of Medicine, St Louis, Mo. Received April 12, 2022; revision requested June 1; revision received October 22; accepted November 14. **Address correspondence to** H.C. (email: *hongchen@wustl.edu*).

A.N. supported by the Radiological Society of North America Research and Education Foundation and Canon Medical Systems USA (RR1953). H.C. supported by the National Institutes of Health (R01EB027223, R01EB030102, R01MH116981). C.P.P. supported by the Cognitive, Computational and Systems Neuroscience Pathway at Washington University in St Louis (NIH T32NS115672).

* A.N. and H.C. are co-senior authors.

Conflicts of interest are listed at the end of this article.

See also the editorial by Fowlkes in this issue.

Radiology 2023; 307(2):e 220869 • https://doi.org/10.1148/radiol.220869 • Content code: NR

Background: Neurodegenerative disorders (such as Alzheimer disease) characterized by the deposition of various pathogenic forms of tau protein in the brain are collectively referred to as tauopathies. Identification of the molecular drivers and pathways of neurodegeneration is critical to individualized targeted treatment of these disorders. However, despite important advances in fluid biomarker detection, characterization of these molecular subtypes is limited by the blood-brain barrier.

Purpose: To evaluate the feasibility and safety of focused ultrasound–mediated liquid biopsy (sonobiopsy) in the detection of brain-derived protein biomarkers in a transgenic mouse model of tauopathy (PS19 mice).

Materials and Methods: Sonobiopsy was performed by sonicating the cerebral hemisphere in 2-month-old PS19 and wild-type mice, followed by measurement of plasma phosphorylated tau (p-tau) species (30 minutes after sonication in the sonobiopsy group). Next, spatially targeted sonobiopsy was performed by sonicating either the cerebral cortex or the hippocampus in 6-month-old PS19 mice. To detect changes in plasma neurofilament light chain (a biomarker of neurodegeneration) levels, blood samples were collected before and after sonication (15 and 45–60 minutes after sonication). Histologic staining was performed to evaluate tissue damage after sonobiopsy. The Shapiro-Wilk test, unpaired and paired *t* tests, and the Mann-Whitney *U* test were used.

Results: In the 2-month-old mice, sonobiopsy significantly increased the normalized levels of plasma p-tau species compared with the conventional blood-based liquid biopsy (p-tau-181–to–mouse tau [m-tau] ratio: 1.7-fold increase, $P = .006$; p-tau-231–to–m-tau ratio: 1.4-fold increase, $P = .048$). In the 6-month-old PS19 mice, spatially targeted sonobiopsy resulted in a 2.3-fold increase in plasma neurofilament light chain after sonication of the hippocampus and cerebral cortex ($P < .001$). After optimization of the sonobiopsy parameters, no excess microhemorrhage was observed in the treated cerebral hemisphere compared with the contralateral side.

Conclusion: This study showed the feasibility of sonobiopsy to release phosphorylated tau species and neurofilament light chain to the blood circulation, potentially facilitating diagnosis of neurodegenerative disorders.

Supplemental material is available for this article.

A hallmark of Alzheimer disease and other tauopathies is the hyperphosphorylation of tau species in the brain (1), which leads to their dissociation from the microtubule, misfolding, aggregation, and subsequent neuronal death. Interindividual variations in the posttranslational modifications of tau species have been associated with disease stage and pathogenicity (1,2). In recent years, various PET radiotracers for amyloid and tau imaging and highly sensitive biofluid markers have emerged for Alzheimer disease (3,4); however, accurate and comprehensive characterization of the complex landscape of brain proteinopathies with their secondary neurodegenerative effects remains challenging. Noninvasive detection of brain-derived pathogenic tau molecules and biomarkers of neurodegeneration is imperative to advance the understanding of tauopathies and develop personalized therapeutic strategies.

Recently, highly sensitive cerebrospinal fluid and blood-based liquid biopsy (BLBx) assays have been developed to detect fluid biomarkers of primary proteinopathy and secondary biomarkers that herald downstream processes in neurodegenerative disorders (5,6). Neurofilament light chain (NfL) protein is one of the emerging secondary biomarkers that is released from damaged axons into the extracellular space and subsequently into the bloodstream (7) and has shown promise in the prediction of disease progression (8). However, beyond screening for early detection of neurodegenerative disorders, the clinical utility of these blood-based biomarkers faces crucial challenges. First, the blood-brain barrier (BBB) acts as a biased filter with differential permeability to brain-derived biomarkers, which allows the passage of certain protein biomarkers while limiting the release of various other pathogenic protein species into the

Abbreviations

BBB = blood-brain barrier, BLBx = blood-based liquid biopsy, m-tau = mouse tau, NfL = neurofilament light chain, p-tau = phosphorylated tau, p-tau-181 = p-tau at threonine position 181, p-tau-231 = p-tau at threonine position 231

Summary

Focused ultrasound–mediated blood-based liquid biopsy (sonobiopsy) improves detection of biomarkers of neurodegeneration from spatially targeted brain regions into the blood circulation compared with liquid biopsy without focused ultrasound.

Key Results

- In a tauopathy mouse model, focused ultrasound–mediated liquid biopsy (sonobiopsy) significantly increased the level of normalized phosphorylated tau at threonine position 181 (1.7-fold increase, $P = .006$) and, to a lesser extent, the level of normalized phosphorylated tau at threonine position 231 (1.4-fold increase, $P = .048$) compared with levels in the control mouse group that underwent liquid biopsy without focused ultrasound.
- Spatially targeted sonobiopsy resulted in a 2.3-fold increase in plasma neurofilament light chain ($P < .001$).

circulation (9,10). Second, fluid biomarkers lack anatomic information on the location of the disease. Accordingly, variations in disease-related brain-derived biomarkers can be obscured by their release from peripheral tissues or nonspecific release from normal brain tissue. Therefore, conventional approaches are unable to colocalize the source of biomarker release with observed neuroimaging abnormalities, which is key to establish the underlying molecular pathways driving the neurodegenerative changes. Lastly, rapid clearance of biomarkers from biofluids may render them undetectable. In addition, the variability caused by inter- or intraindividual differences in clearance rates could limit the accuracy of fluid biomarker approaches.

Focused ultrasound–mediated blood-based liquid biopsy (sonobiopsy) is an emerging technique that has the promise to address these challenges. Localized focused ultrasound (with a focal region size on the order of a few millimeters) combined with microbubbles can disrupt the BBB that is visible with contrast-enhanced MRI (11) and can facilitate drug delivery in the brain (12). Sonobiopsy leverages this targeted reversible focal opening of the BBB to increase the diagnostic yield of plasma biomarkers originating from the anatomically targeted brain location (ie, spatially selective). By collecting blood samples immediately before and after sonobiopsy, the postsonobiopsy biomarker levels can be compared against baseline levels to provide a direct estimate of focused ultrasound–induced release from the sonicated brain region (ie, temporally controlled).

Our group and others have used sonobiopsy to facilitate the release of nucleic acid–based biomarkers from brain tumors and brain-derived tissue markers from the healthy brain parenchyma to the bloodstream (13–18). Here, we hypothesized that the application of sonobiopsy can be extended to neurodegenerative diseases by enhancing the release of pathologic tau proteins and markers of neurodegeneration to the blood. In this proof-of-principle study, we sought to determine the capability of sonobiopsy to release phosphorylated tau species (p-tau) and NfL into the bloodstream by opening the BBB.

Materials and Methods

Animal Preparation

Male transgenic PS19 (B6;C3-Tg (Prnp-MAPT*P301S) PS19Vle/J mice expressing P301S human tau) and noncarrier wild-type mice were purchased from the Jackson Laboratory (stock no. 008169) (19). All animal procedures were reviewed and approved by the institutional animal care and use committee at Washington University in St Louis in accordance with the Guide for the Care and Use of Laboratory Animals and the Animal Welfare Act.

Focused Ultrasound Set-Up, Sonobiopsy Procedures, and Study Designs

The MRI-compatible focused ultrasound system (Fig 1A) used in this study has been previously described (16,20). Details of the focused ultrasound set-up, MRI, microbubble preparation, passive cavitation detection, and assessment of BBB opening are provided in Appendix S1. Briefly, microbubbles were injected 30 seconds prior to the start of focused ultrasound sonication (frequency, 1.5 MHz; peak negative pressure after derating for skull attenuation, 0.68 MPa; pulse repetition frequency, 5 Hz; duty cycle, 3.35%; pulse length, 6.7 msec; treatment duration, 32 seconds).

In the first experiment, 15 PS19 and 13 wild-type 2-month-old mice were divided into sonobiopsy (seven PS19 mice, seven wild-type mice) and control BLBx (eight PS19 mice, six wild-type mice) groups. Focused ultrasound was applied to the right cerebral hemisphere (Fig 1B), which includes areas that exhibit early p-tau deposition in young PS19 mice (ie, hippocampus, piriform cortex, and entorhinal cortex) (21,22). Blood samples were collected via cardiac puncture 30 minutes after focused ultrasound sonication in the sonobiopsy groups or sham treatment in the BLBx groups. The plasma levels of p-tau species phosphorylated at threonine-181 (p-tau-181) and threonine-231 (p-tau-231) (19,23) were measured in focused ultrasound–treated and BLBx PS19 and wild-type mice. In addition, the plasma levels of mouse tau (total m-tau) were measured as an internal control to normalize p-tau levels in plasma (refer to Appendix S1 for details on p-tau normalization).

In the second experiment, a lower peak negative pressure was applied (0.40 MPa vs 0.68 MPa in the first experiment), and smaller brain areas were targeted. Otherwise, the same sonication parameters were used. Fourteen 6-month-old PS19 mice were divided into control BLBx ($n = 5$) and sonobiopsy ($n = 9$) groups. Focused ultrasound sonication was performed at either the ventral anterolateral cerebral cortex (ie, olfactory cerebral cortex that includes the piriform cortex and amygdala; $n = 3$) or the hippocampus ($n = 6$) (Fig 2). Both brain regions exhibit early neurodegenerative changes in PS19 mice (19,23). The selection of a smaller target region of the brain enabled examination of the regional specificity of sonobiopsy by evaluating the biomarker release from each localized region. To mitigate the effects of variabilities in baseline plasma biomarkers among the PS19 mice, a pre-post study design was adopted to evaluate changes in NfL levels by sampling blood before focused ultrasound (pre-focused ultrasound, submandibular

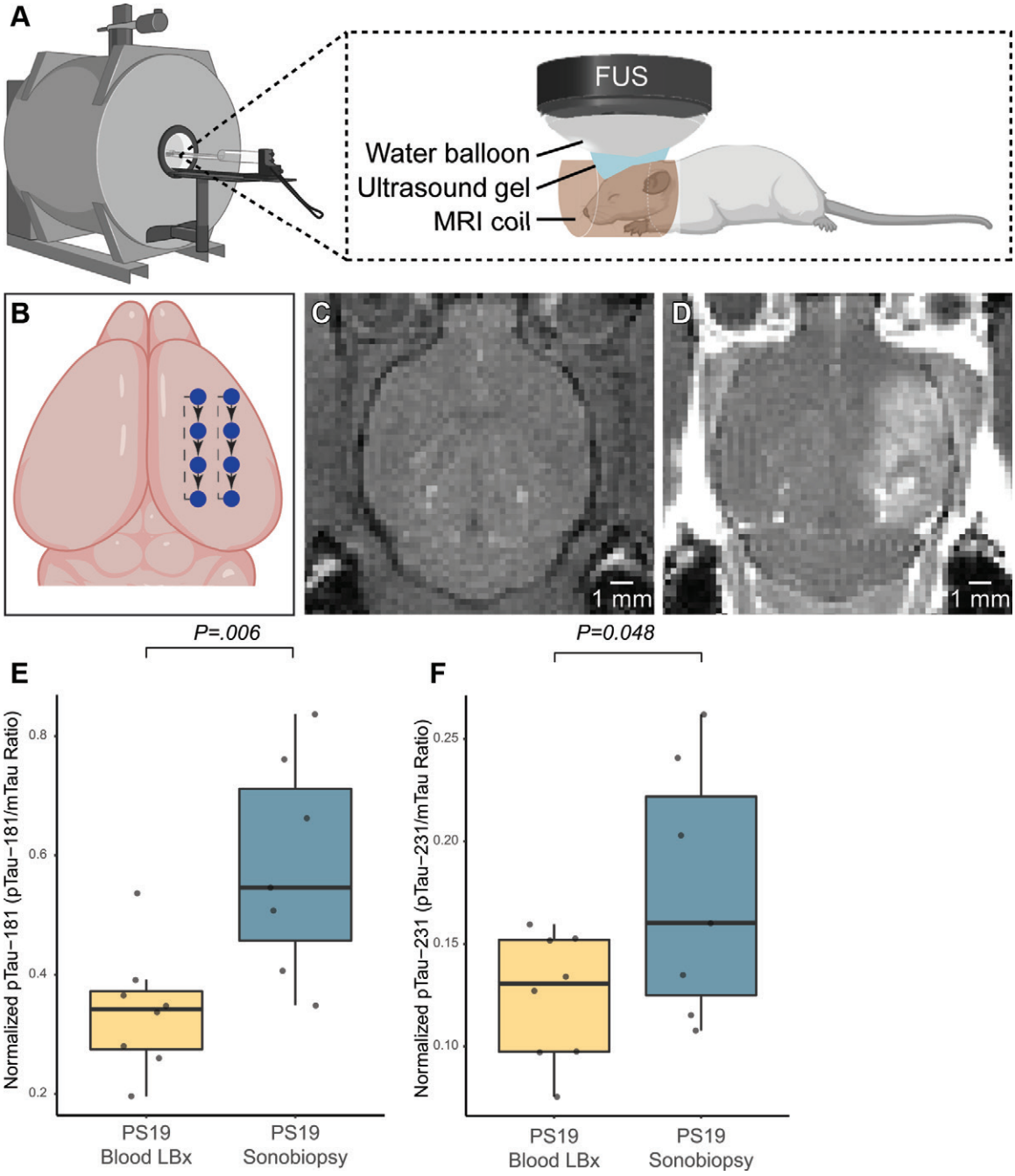

Figure 1: MRI-guided sonobiopsy changed composition of circulating phosphorylated tau (p-tau) species in 2-month-old PS19 mice (experiment 1). **(A)** Diagram of the focused ultrasound (FUS) system in the small-animal MRI scanner. The mouse head was fixed in the MRI coil, and the focused ultrasound transducer was coupled to the skull with ultrasound gel and a water balloon filled with degassed water. **(B)** Schematic of the focused ultrasound trajectory targeting the right cerebral hemisphere. **(C)** T1-weighted MRI scans were acquired before focused ultrasound and intravenous contrast material administration. **(D)** Post-focused ultrasound/postcontrast T1-weighted MRI scans confirmed focused ultrasound–induced blood-brain barrier (BBB) disruption as a signal enhancement. Except for one wild-type mouse, successful BBB opening was observed in all mice that underwent focused ultrasound (six of seven wild-type mice, seven of seven PS19 mice). The wild-type mouse with no evidence of BBB opening after focused ultrasound was excluded from further analysis. There was no significant group difference ($P = .71$) in the volume of focused ultrasound–mediated BBB opening between PS19 (mean, 30.88 mm^3 ± 17.94 [SD]) and wild-type (35.12 mm^3 ± 22.94) mice. **(E)** In PS19 mice, normalized p-tau-181 (p-tau-181–to–m-tau ratio) was significantly greater ($P = .006$) in the sonobiopsy group ($n = 7$; mean, 0.57 ± 0.19) compared with the normalized pTau-181 in the blood-based liquid biopsy (blood LBx) group (ie, control group without focused ultrasound treatment; $n = 8$; mean, 0.36 ± 0.09). **(F)** In PS19 mice, the normalized pTau-231 (pTau-231–to–m-tau ratio) was significantly greater ($P = .048$) in the sonobiopsy group ($n = 8$; mean, 0.17 ± 0.06) compared with the normalized pTau-181 in the blood LBx group ($n = 7$; mean, 0.13 ± 0.03). Black bars indicate median in **E** and **F**.

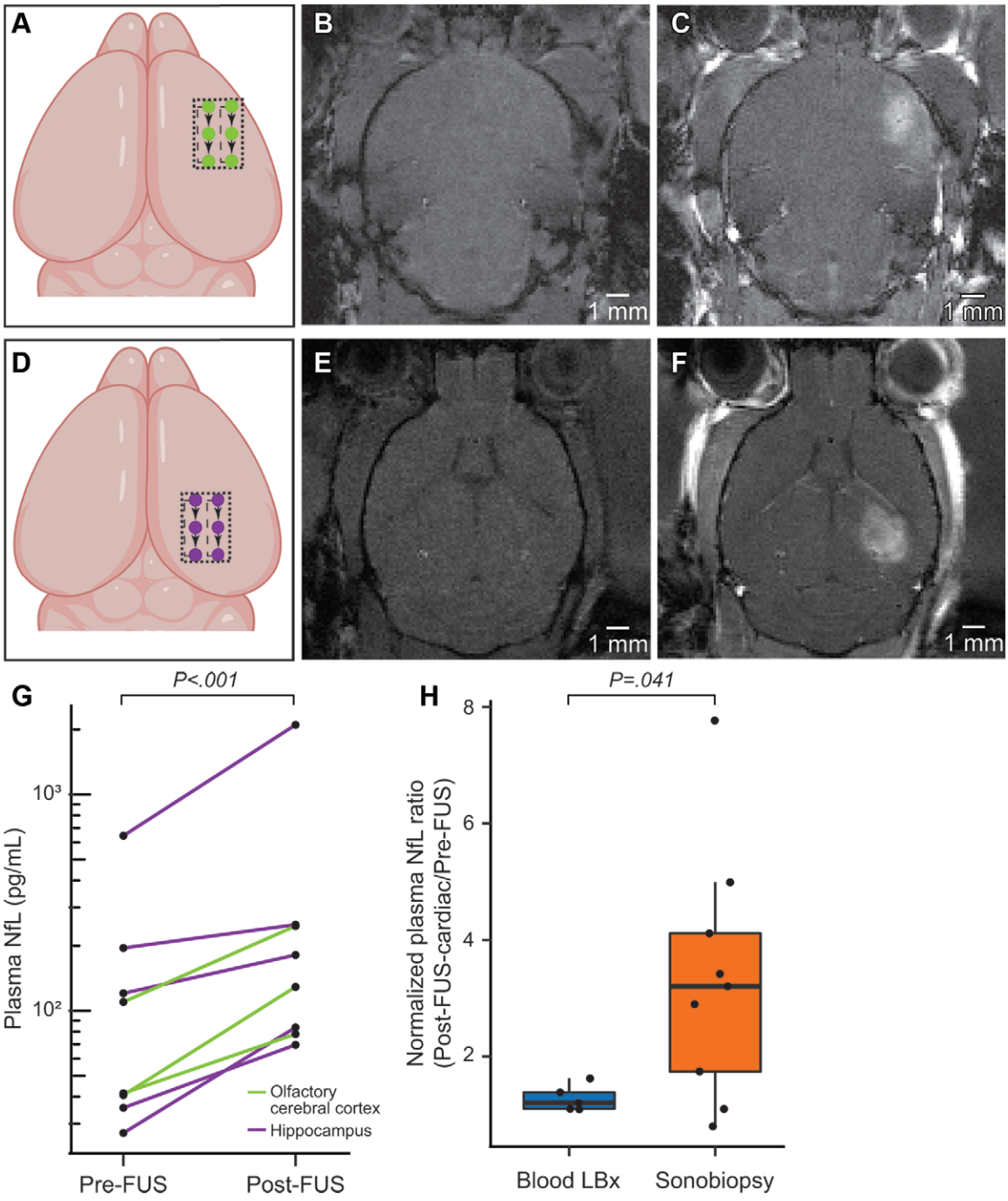

Figure 2: Sonobiopsy enhanced levels of plasma neurofilament light chain protein (NfL) in 6-month-old PS19 mice (experiment 2). **(A)** Schematic of the focused ultrasound trajectory targeting the olfactory cerebral cortex (piriform cortex and amygdala). **(B)** T1-weighted MRI scans were acquired before focused ultrasound and intravenous contrast material administration. **(C)** Post-focused ultrasound and postcontrast T1-weighted MRI scans enabled confirmation of focused ultrasound-induced blood-brain barrier (BBB) disruption as a signal enhancement. **(D)** Schematic of the focused ultrasound trajectory targeting the hippocampus. **(E)** T1-weighted MRI scans were acquired before focused ultrasound and intravenous contrast material administration. **(F)** Post-focused ultrasound and postcontrast T1-weighted MRI scans enabled confirmation of focused ultrasound–induced BBB disruption as a signal enhancement. There was no significant difference ($P = .17$) in the volume of focused ultrasound–mediated BBB disruption between mice treated at the olfactory cerebral cortex (mean, 21.74 $mm^3 \pm 5.81$) or the hippocampus (mean, 15.42 $mm^3 \pm 5.83$). **(G)** Sonobiopsy resulted in a 2.3-fold increase in plasma NfL levels ($n = 8$, $P < .001$). **(H)** The normalized plasma NfL (post-focused ultrasound–to–pre-focused ultrasound ratio) was significantly greater ($P = .041$) in the sonobiopsy group ($n = 9$, 3.34 ± 2.15) than the blood LBx group (control group without focused ultrasound treatment, $n = 5$; 1.28 ± 0.22). Black bar indicates median.

blood collection), 15 minutes after focused ultrasound (post-focused ultrasound, submandibular blood collection), and 45–60 minutes after focused ultrasound (post-focused ultrasound–cardiac, terminal cardiac puncture). In the BLBx group, submandibular blood collection (pre-focused ultrasound) was followed by cardiac puncture (post-focused ultrasound–cardiac). Unlike the post-focused ultrasound–cardiac samples, NfL measurements of pre-focused ultrasound and post-focused ultrasound blood samples in the group that underwent focused ultrasound are directly comparable (same blood collection method and NfL measurements in the same batch of reagents with the same sample dilutions) (Table S1).

The sonication trajectories for both experiments are shown in Figures 1 and 2 and are discussed in Appendix S1. Contrast-enhanced T1-weighted MRI was performed to assess BBB disruption (Figs 1, 2). Mice in the BLBx groups underwent a sham sonobiopsy procedure, including pre-focused ultrasound and post-focused ultrasound MRI scans, saline injection, and no focused ultrasound sonication.

Plasma Biomarker Detection

Mouse blood was collected into ethylenediaminetetraacetic acid (EDTA) tubes and spun at 6000 g for 5 minutes at 4°C. The top plasma layer was transferred to a 0.5-mL microcentrifuge tube and stored at −80°C. All plasma protein measurements were performed in duplicate on a fully automated HD-X Analyzer (Quanterix) using ultrahigh sensitive Single Molecule Array (Simoa) kits. Details and plasma sample dilutions for all assays are provided in Table S1.

Histologic Analysis

Hematoxylin-eosin staining was performed to examine red blood cell extravasation and cellular injury. In the first experiment, brain tissue slices were collected from one PS19 mouse and seven wild-type mice. For the second experiment, brain tissue slices were also available from four additional PS19 mice that were sonicated using the same conditions, resulting in a total sample size of 13. Tissue slices were imaged on the Axio Scan.Z1 Slide Scanner (Zeiss). QuPath, version 0.2.0 (24) was used to detect the presence of focused ultrasound–induced hemorrhage (see Appendix S1 for further details).

Statistical Analysis

All statistical analyses were performed using R, version 4.1.2 *(https://www.r-project.org/)*. All continuous variables were tested for normal distribution using the Shapiro-Wilk test (Table S2). All absolute plasma levels were log-transformed to achieve a normal distribution, while the plasma level ratios were compared with no transformation (see Appendix S1 for further details). For normally distributed parameters, *t* tests were used for between-group comparisons, assuming unequal variance. The Mann-Whitney *U* test was used for parameters deviating from normal distribution. Paired *t* tests were conducted to compare pre- and postsonication levels of NfL and ipsi- and contralateral microhemorrhage density. As we expected increases in biomarker levels after focused ultrasound treatment and tissue microhemorrhage density in the side treated with focused ultrasound, all reported *P* values are one tailed, unless otherwise specified ($P < .05$ indicated a significant difference).

Results

Sonobiopsy and Circulating P-Tau Species in PS19 Mice

We first demonstrated the efficacy of sonobiopsy to enrich the blood with pathologic p-tau species compared with conventional BLBx. As expected, the absolute levels of p-tau species were higher in PS19 mice than in wild-type mice (Fig S1). Although the absolute levels of p-tau species were not significantly higher in the PS19 mice that underwent focused ultrasound (Fig S1), there was a significant 1.7-fold increase ($P < .001$) in the normalized levels of p-tau-181 (ie, p-tau-181–to–m-tau ratio) in the seven PS19 mice that underwent sonobiopsy (mean, 0.58 ± 0.18 [SD]) compared with the eight PS19 mice that underwent BLBx (mean, 0.34 ± 0.10) (Fig 1E). There was a significant 1.4-fold increase ($P = .048$) in the normalized levels of p-tau-231 (p-tau-231–to–m-tau ratio) in the seven PS19 mice that underwent sonobiopsy (mean, 0.17 ± 0.06) compared with the eight PS19 mice that underwent BLBx (mean, 0.12 ± 0.03) (Fig 1F). Unlike the PS19 mice, there was no significant increase in normalized p-tau-181 or p-tau-231 levels between the sonobiopsy ($n = 6$) and BLBx ($n = 6$) groups for the wild-type mice (Fig S2).

Sonobiopsy and NfL in the Early Neurodegenerative Stage of PS19 Mice

We further evaluated the capability of sonobiopsy to release NfL, a secondary biomarker of tauopathy, in the early neurodegenerative stages in 6-month-old PS19 mice (19). We also assessed the potential of survival blood collection and the capability to target specific brain regions. There was a 2.3-fold increase in plasma NfL after focused ultrasound (post-focused ultrasound vs pre-focused ultrasound [$n = 8$]; both submandibular blood collections, $P < .001$; Fig 2G). Next, we calculated the normalized plasma NfL level using the ratio of plasma NfL levels in the terminal cardiac sample (post-focused ultrasound–cardiac) to the pre-focused ultrasound submandibular sample (pre-focused ultrasound). Compared with the BLBx group (untreated PS19 mice), the ratio of post-focused ultrasound–cardiac to pre-focused ultrasound plasma NfL level was 2.6-fold higher in the PS19 mice that underwent sonobiopsy (Mann-Whitney *U* test given nonnormal distribution; $P = .041$; mice that underwent sonobiopsy, 3.34 ± 2.15 [$n = 9$]; mice that underwent BLBx, 1.28 ± 0.22 [$n = 5$]) (Fig 2H). There was no clear difference in focused ultrasound-induced NfL release between the hippocampus and cortex in sonicated groups (Fig 2G). Altogether, by accounting for the baseline levels of plasma NfL, our findings show that sonication of the hippocampus and cerebral cortex leads to an increase in NfL plasma levels in the PS19 mice, even at an early neurodegenerative stage.

Assessment of Brain Injury with Sonobiopsy

Hematoxylin-eosin staining of the eight 2-month-old PS19 mice treated with 0.68 MPa (Fig 3A) revealed that the microhemorrhage surface area in the hemisphere treated with focused

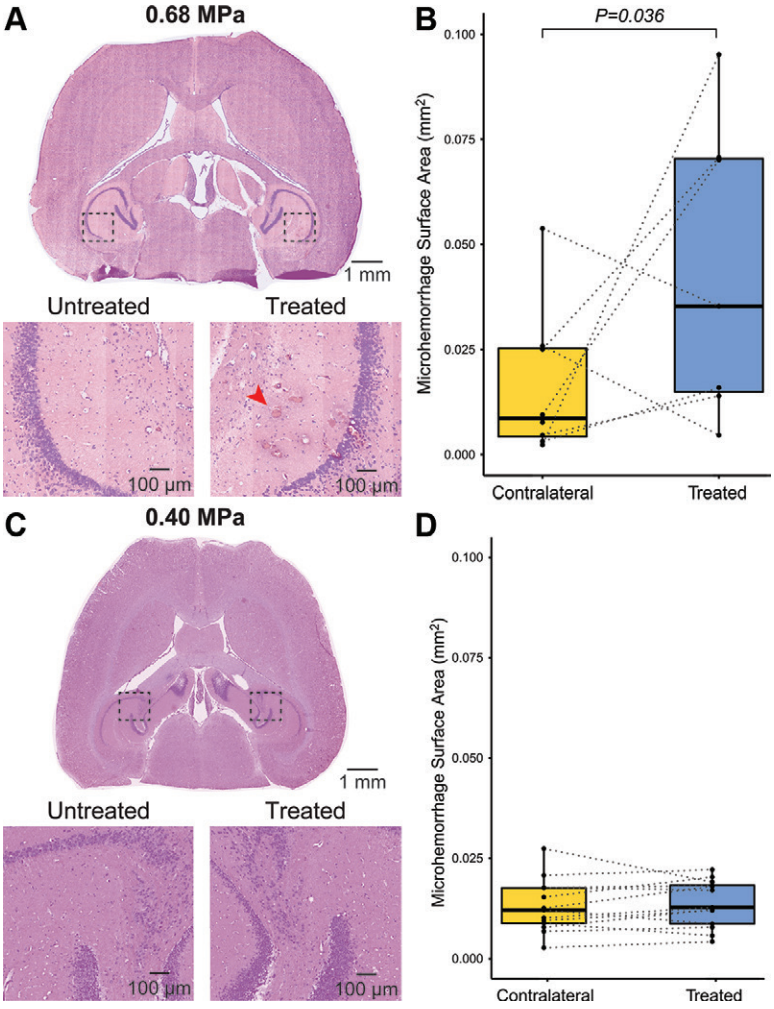

Figure 3: Safety assessment of sonobiopsy. **(A)** Representative hematoxylin-eosin staining for experiment 1 with 2-month-old mice. **(B)** There was a significant increase in microhemorrhage surface area (red arrow) in the treated hemisphere (mean, 0.051 mm^2 ± 0.039) compared with the untreated hemisphere (mean, 0.016 mm^2 ± 0.018; P = .036). **(C)** Representative hematoxylin-eosin staining for experiment 2 with 6-month-old mice. **(D)** There was no significant difference in the microhemorrhage density in the treated hemisphere (mean, 0.014 mm^2 ± 0.006) compared with the untreated hemisphere (mean, 0.013 mm^2 ± 0.007; P = .26; n = 13). Minimal visualized microhemorrhage in the untreated contralateral cerebral hemisphere likely represents artifactual red blood cell extravasation during perfusion, tissue handling, and fixation.

ultrasound (mean, 0.051 mm^2 ± 0.039) was significantly greater than that in the untreated contralateral hemisphere (mean, 0.016 mm^2 ± 0.018; P = .036) (Fig 3B). For the 13 6-month-old PS19 mice that were treated with the lower focused ultrasound peak negative pressure (0.40 MPa) and a smaller target region, hematoxylin-eosin staining (Fig 3C) revealed no excess in the microhemorrhage surface area in the hemisphere treated with focused ultrasound (mean, 0.014 mm^2 ± 0.006) compared with the untreated hemisphere (mean, 0.013 mm^2 ± 0.007; P = .26) (Fig 3D). Minimal inertial cavitation (a predictor for focused ultrasound–induced tissue damage) was detected with passive cavitation detection in both experiments (Appendix S1).

Discussion

In this study, sonobiopsy significantly enhanced the release of p-tau species and a secondary marker of neurodegeneration into the bloodstream for noninvasive diagnosis of tauopathies and neurodegenerative diseases. Sonobiopsy leveraged the spatial targeting of focused ultrasound to open a relatively small region of the brain, thus allowing for spatially localized biomarker release. Finally, we showed that sonobiopsy of brain parenchyma is safe, and brain damage (ie, microhemorrhage) can be minimized by lowering the peak negative pressure of focused ultrasound, while maintaining elevated blood levels of biomarkers beyond baseline measurements.

Previously, sonobiopsy enabled sensitive detection of circulating biomarkers by enriching the blood samples of mouse and pig glioma models with DNA- or RNA-based biomarkers (13,14,16,18). However, the BBB is inherently compromised by tumor growth in these brain tumor models. A prior study showed the application of sonobiopsy to release normal structural brain proteins in the healthy pig model (15). This study expanded the utility of sonobiopsy by demonstrating the focused ultrasound–induced release of both primary pathogenic proteins (p-tau species) and a downstream biomarker of neurodegeneration. Moreover, we showed that enrichment of plasma with p-tau species after focused ultrasound occurred exclusively in PS19 mice but not in wild-type mice. This finding supports the belief that sonobiopsy-induced release of brain-derived biomarkers is specific to the underlying disease in the focused ultrasound–targeted brain tissue.

We observed high baseline levels of p-tau-181, p-tau-231, and NfL in PS19 mice. This is expected, as these are established biomarkers for tauopathy and neurodegeneration that are readily detectable in plasma with highly sensitive assays. Despite the likely dampening of the apparent yield of sonobiopsy, the 1.4–2.3-fold increases in p-tau species and NfL suggest that sonobiopsy is robust and can have a clinical impact, even with biomarkers with relatively high baseline levels and intra- or interindividual variability (25,26). It follows that sonobiopsy will have a much higher yield for low-abundance peripheral biomarkers, such as DNA- or RNA-based biomarkers (13,16). To further complicate diagnostic performance, p-tau-181, p-tau-231, and NfL had large variabilities across subjects, which likely reflects the heterogeneity observed in neuropathology in PS19 mice (27). Moreover, interindividual variations in nonspecific release and clearance of biomarkers can result in large differences in baseline levels of brain-derived plasma biomarkers in the steady state. Similarly, in the clinical setting, such variations that are unrelated to the underlying disease process can decrease the sensitivity and specificity of plasma biomarkers in conventional liquid biopsy. In contrast, sonobiopsy can directly address this limitation by allowing blood sample collection before and after sonication to compare the biomarker levels within each subject. In this way, the

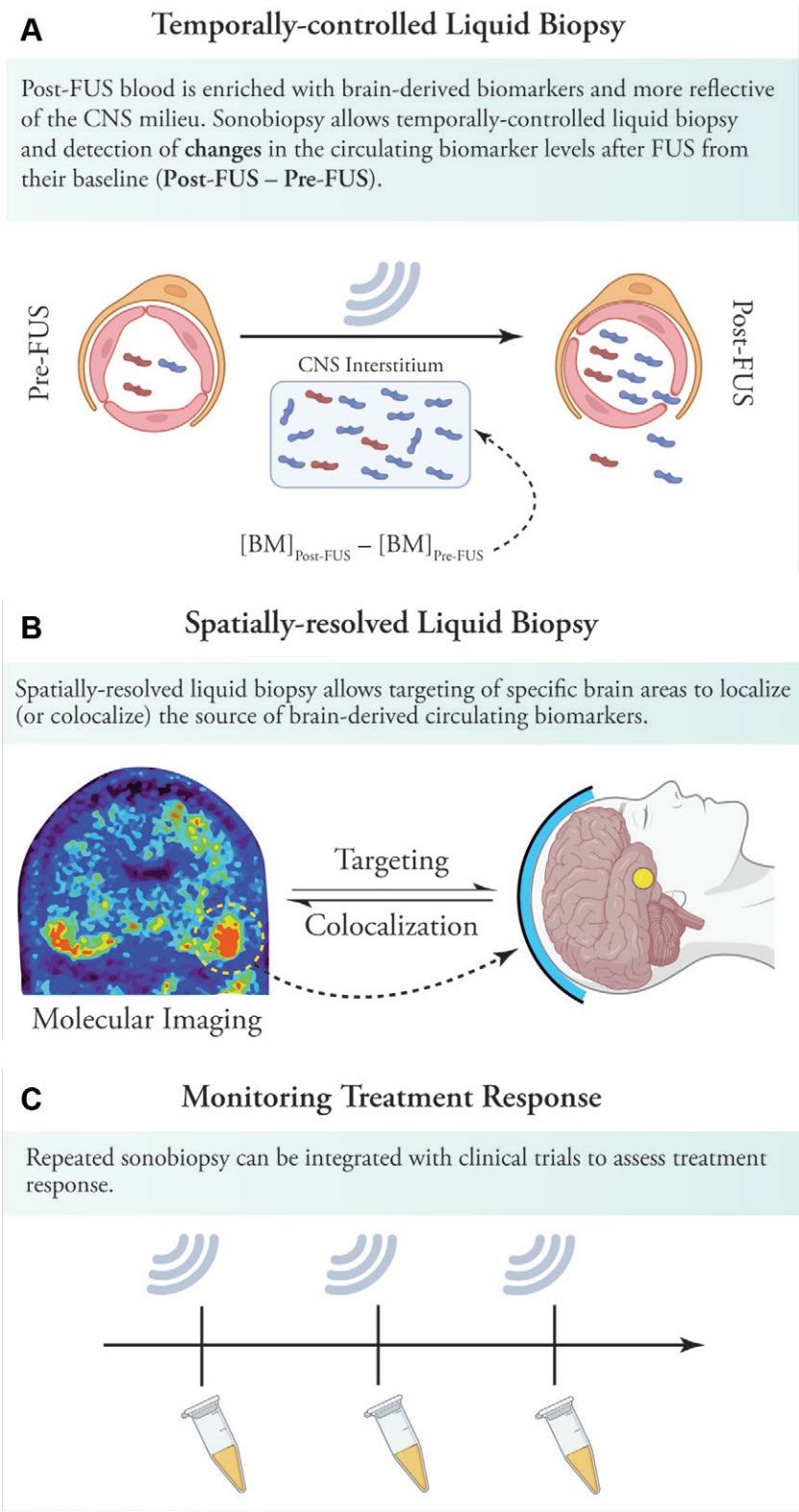

Figure 4: Implications of sonobiopsy in clinical settings. **(A)** By opening the blood-brain barrier (BBB) and releasing proteins from the brain into the circulation, sonobiopsy can enrich plasma with brain-derived pathologic protein species. By simply collecting blood samples before and after sonications, sonobiopsy enables temporally controlled liquid biopsy and detection of changes in circulating pathologic protein species and other biomarkers after focused ultrasound. **(B)** Sonobiopsy can allow spatially resolved liquid biopsy. This can, in turn, be used for targeted BBB opening in brain areas with high protein deposits on molecular imaging (eg, tau or amyloid PET imaging). Sonobiopsy of these brain areas could shed light on the dominant pathogenic subtypes in heavily involved brain areas. In addition, the release of abnormal specific protein species can be colocalized to the brain regions showing the greatest metabolic, structural, or microstructural deficits. This can help identify the main culprits in pathogenesis of various neurodegenerative disorders. **(C)** Sonobiopsy can be readily integrated into focused ultrasound–induced BBB opening clinical trials to allow monitoring of treatment response by assessing changes in brain-derived pathogenic proteins. BBB = blood-brain barrier, BM = biomarker concentration in plasma, CNS = central nervous system, FUS = focused ultrasound.

changes in plasma biomarker levels from their baseline after sonication can be used to directly estimate focused ultrasound–induced release of brain-derived biomarkers from the targeted area in the brain.

The observed microhemorrhage (Fig 3A) can be minimized by lowering the peak negative pressure (Fig 3C) while still achieving sonobiopsy-induced biomarker release (Fig 2G). Although the higher peak negative pressure increases the efficacy of sonobiopsy (14,28), the efficacy likely varies depending on the biomarker molecular properties, including sizes and the kinetics of biomarker influx into and clearance from the plasma (18). For example, sonobiopsy at 0.40 and 0.68 MPa successfully increased plasma levels of the protein biomarkers tau and NfL, which have circulation half-lives of approximately 10 hours and several weeks, respectively (29). We expect that a balance between the safety and efficacy of sonobiopsy can be achieved by optimizing the focused ultrasound parameters, target volume, and plasma sampling times for the biomarker of interest and the targeted tissue. A thorough investigation of the relationship between focused ultrasound parameters and the released biomarker properties is warranted in future work.

Although sonobiopsy was effective when targeting specific brain regions (ie, the hippocampus or the olfactory cerebral cortex), there was no significant difference in NfL levels between these specific brain regions. This may be explained by early neurodegenerative changes in both targeted areas in PS19 mice (19,23). Future studies that use a negative control design to target brain areas that are resilient to neurodegeneration are necessary to further examine spatial specificity of sonobiopsy.

This proof-of-concept feasibility study had several limitations. First, this study showed that sonobiopsy could result in a quantitative increase in the normalized p-tau levels. Future studies are needed to examine the qualitative effects of sonobiopsy on plasma biomarkers with an in-depth analysis of posttranslational modifications, size distribution, and oligomerization. Second, while this study showed that sonobiopsy could be successfully performed with relatively low focused ultrasound acoustic pressures (0.40 MPa) in the mouse model, we did not perform a comprehensive optimization study to characterize the effects of focused ultrasound parameters and determine the optimal blood collection time. While these effects have been described in different settings and macromolecules (RNA or DNA) (14,18), it is conceivable that the dynamics and kinetics of sonobiopsy would be different for protein biomarkers. Future studies can use cavitation monitoring (30), quantitative BBB permeability assessment with dynamic contrast-enhanced MRI (31), and long-term behavioral analysis to optimize the focused ultrasound parameters for safe and effective sonobiopsy. Third, in this study, we did not include focused ultrasound–only or microbubble-only control groups. Lastly, this study focused on proteins with relatively small molecular weights (48–68 kDa). Future studies are needed to determine the generalizability of sonobiopsy in releasing larger brain-derived protein biomarkers.

Our findings and potential translatability of sonobiopsy should be interpreted and assessed with caution, given the vast differences in brain anatomy and skull thickness between mice and humans. However, recent MRI-guided focused ultrasound studies have shown the safety of BBB opening in patients with neurodegenerative disorders such as Alzheimer disease (32,33) and large-volume BBB disruption in patients with glioblastoma (34). Apart from enhancing liquid biopsy by increasing plasma levels of various biomarkers, our proof-of-principle study has important translational implications (Fig 4). First, sonobiopsy can release brain-derived subtypes of abnormal protein species into the bloodstream. By allowing temporally controlled liquid biopsy, changes in biomarker levels (from baseline levels) can provide a window into the molecular derangements in the central nervous system milieu. Second, the spatial resolution of sonobiopsy can be leveraged to colocalize the biomarkers released by sonobiopsy with nonspecific imaging biomarkers of neurodegeneration, such as decreased metabolism or tissue microstructural deficits. Further, sonobiopsy can combine the spatial resolution of PET radiotracers with the molecular resolution of fluid biomarkers. For instance, sonobiopsy can be used to probe the individual patterns of tau phosphorylation as well as the secondary neurodegenerative effects of tauopathy by targeting the brain areas with a high burden of tau deposits on tau PET images. Third, repeated sonobiopsy before and after treatment can be used in the clinic to perform temporally controlled liquid biopsy to monitor treatment response.

In conclusion, this study showed the feasibility and safety of sonobiopsy to enhance the detection of both biomarkers of the primary pathogenic process (eg, posttranslational modifications of the tau protein) and secondary neurodegeneration. This proof-of-principle study was the first to open the door for noninvasive and spatially targeted diagnosis and monitoring of neurodegenerative disorders with sonobiopsy.

Acknowledgments: The MRI-guided experiments presented in this work were performed at the Small Animal Magnetic Resonance Facility of the Mallinckrodt Institute of Radiology, Washington University in St Louis.

Author contributions: Guarantors of integrity of entire study, **C.P.P., A.N., H.C.**; study concepts/study design or data acquisition or data analysis/interpretation, all authors; manuscript drafting or manuscript revision for important intellectual content, all authors; approval of final version of submitted manuscript, all authors; agrees to ensure any questions related to the work are appropriately resolved, all authors; literature research, **C.P.P., E.C.L., T.L.S.B., A.N., H.C.**; experimental studies, **C.P.P., J.Y., Y.Y., E.C.L., A.N., H.C.**; statistical analysis, **C.P.P., A.N.**; and manuscript editing, **C.P.P., J.Y., E.C.L., T.L.S.B., A.N., H.C.**

Disclosures of conflicts of interest: **C.P.P.** No relevant relationships. **J.Y.** No relevant relationships. **Y.Y.** No relevant relationships. **E.C.L.** Royalties from Neurolutions; consultant to Monteris Medical, E15, Acera, Alcyone, Intellectual Ventures, Neurolutions, Osteovantage, Pear Therapeutics, Sante Ventures, Microbot SAB: Pear Therapeutics, Microbot, Petal Surgical; license for intellectual property from Neurolutions, Osteovantage, Caeli Vascular, and Inner Cosmos; licensing and product development agreements or royalties for inventions from Cerovations, Intellectual Ventures, Sora Neuroscience, Inner Cosmos, and Neurolutions; Washington University owns equity in Neurolutions; patents issued to Washington University; stock ownership in Neurolutions, General Sensing, Osteovantage, Face to Face Biometrics, Caeli Vascular, Acera, Sora Neuroscience, Inner Cosmos, Kinetrix, NeuroDev, and Petal Surgical. **T.L.S.B.** Grant from Siemens; consulting fees from Biogen and Eisai; honoraria from Biogen and Eisai; serves on NIH-sponsored DataSafety monitoring boards and advisory boards for Eisai and Biogen; co-chair of the American Society for Neuroradiology Committee on Amyloid Related Imaging Abnormalities; receipt of radiopharmaceutical doses, precursors, and technology transfer from Avid Radiopharmaceuticals, LMI, and Cerveau. **A.N.** No relevant relationships. **H.C.** On the board of directors for the International Society of Therapeutic Ultrasound, member of the Acoustical Society of America Biomedical Ultrasound technical committee, on the IEEE International Ultrasonics technical committee.

References

1. Dujardin S, Commins C, Lathuiliere A, et al. Tau molecular diversity contributes to clinical heterogeneity in Alzheimer's disease. Nat Med 2020;26(8):1256–1263 [Published correction appears in Nat Med 2021;27(2):356.].
2. Wesseling H, Mair W, Kumar M, et al. Tau PTM Profiles Identify Patient Heterogeneity and Stages of Alzheimer's Disease. Cell 2020;183(6):1699–1713.e13.
3. Ossenkoppele R, van der Kant R, Hansson O. Tau biomarkers in Alzheimer's disease: towards implementation in clinical practice and trials. Lancet Neurol 2022;21(8):726–734.
4. Hansson O. Biomarkers for neurodegenerative diseases. Nat Med 2021;27(6):954–963.
5. Thijssen EH, La Joie R, Wolf A, et al; Advancing Research and Treatment for Frontotemporal Lobar Degeneration (ARTFL) investigators. Diagnostic value of plasma phosphorylated tau181 in Alzheimer's disease and frontotemporal lobar degeneration. Nat Med 2020;26(3):387–397.
6. Janelidze S, Mattsson N, Palmqvist S, et al. Plasma P-tau181 in Alzheimer's disease: relationship to other biomarkers, differential diagnosis, neuropathology and longitudinal progression to Alzheimer's dementia. Nat Med 2020;26(3):379–386.
7. Gafson AR, Barthélemy NR, Bomont P, et al. Neurofilaments: neurobiological foundations for biomarker applications. Brain 2020;143(7):1975–1998.
8. Khalil M, Teunissen CE, Otto M, et al. Neurofilaments as biomarkers in neurological disorders. Nat Rev Neurol 2018;14(10):577–589.
9. Hampel H, O'Bryant SE, Molinuevo JL, et al. Blood-based biomarkers for Alzheimer disease: mapping the road to the clinic. Nat Rev Neurol 2018;14(11):639–652.
10. Penner G, Lecocq S, Chopin A, et al. Blood-based diagnostics of Alzheimer's disease. Expert Rev Mol Diagn 2019;19(7):613–621.
11. Hynynen K, McDannold N, Vykhodtseva N, Jolesz FA. Noninvasive MR imaging-guided focal opening of the blood-brain barrier in rabbits. Radiology 2001;220(3):640–646.
12. McMahon D, O'Reilly MA, Hynynen K. Therapeutic Agent Delivery Across the Blood-Brain Barrier Using Focused Ultrasound. Annu Rev Biomed Eng 2021;23(1):89–113.

13. Zhu L, Cheng G, Ye D, et al. Focused Ultrasound-enabled Brain Tumor Liquid Biopsy. Sci Rep 2018;8(1):6553.
14. Zhu L, Nazeri A, Pacia CP, Yue Y, Chen H. Focused ultrasound for safe and effective release of brain tumor biomarkers into the peripheral circulation. PLoS One 2020;15(6):e0234182.
15. Pacia CP, Zhu L, Yang Y, et al. Feasibility and safety of focused ultrasound-enabled liquid biopsy in the brain of a porcine model. Sci Rep 2020;10(1):7449.
16. Pacia CP, Yuan J, Yue Y, et al. Sonobiopsy for minimally invasive, spatiotemporally-controlled, and sensitive detection of glioblastoma-derived circulating tumor DNA. Theranostics 2022;12(1):362–378.
17. Meng Y, Pople CB, Suppiah S, et al. MR-guided focused ultrasound liquid biopsy enriches circulating biomarkers in patients with brain tumors. Neuro Oncol 2021;23(10):1789–1797.
18. Zhang DY, Gould A, Happ HC, et al. Ultrasound-mediated blood-brain barrier opening increases cell-free DNA in a time dependent manner. Neurooncol Adv 2021;3(1):vdab165.
19. Yoshiyama Y, Higuchi M, Zhang B, et al. Synapse loss and microglial activation precede tangles in a P301S tauopathy mouse model. Neuron 2007;53(3):337–351.
20. Yang Y, Pacia CP, Ye D, Yue Y, Chien CY, Chen H. Static Magnetic Fields Dampen Focused Ultrasound-mediated Blood-Brain Barrier Opening. Radiology 2021;300(3):681–689.
21. López-González I, Aso E, Carmona M, et al. Neuroinflammatory Gene Regulation, Mitochondrial Function, Oxidative Stress, and Brain Lipid Modifications With Disease Progression in Tau P301S Transgenic Mice as a Model of Frontotemporal Lobar Degeneration-Tau. J Neuropathol Exp Neurol 2015;74(10):975–999.
22. Sun Y, Guo Y, Feng X, et al. The behavioural and neuropathologic sexual dimorphism and absence of MIP-3α in tau P301S mouse model of Alzheimer's disease. J Neuroinflammation 2020;17(1):72.
23. Gratuze M, Leyns CE, Sauerbeck AD, et al. Impact of TREM2R47H variant on tau pathology-induced gliosis and neurodegeneration. J Clin Invest 2020;130(9):4954–4968.
24. Bankhead P, Loughrey MB, Fernández JA, et al. QuPath: Open source software for digital pathology image analysis. Sci Rep 2017;7(1):16878.
25. Leuzy A, Cullen NC, Mattsson-Carlgren N, Hansson O. Current advances in plasma and cerebrospinal fluid biomarkers in Alzheimer's disease. Curr Opin Neurol 2021;34(2):266–274.
26. Bridel C, Verberk IMW, Heijst JJA, Killestein J, Teunissen CE. Variations in consecutive serum neurofilament light levels in healthy controls and multiple sclerosis patients. Mult Scler Relat Disord 2021;47:102666.
27. Woerman AL, Patel S, Kazmi SA, et al. Kinetics of Human Mutant Tau Prion Formation in the Brains of 2 Transgenic Mouse Lines. JAMA Neurol 2017;74(12):1464–1472.
28. Chen S, Nazeri A, Baek H, et al. A review of bioeffects induced by focused ultrasound combined with microbubbles on the neurovascular unit. J Cereb Blood Flow Metab 2022;42(1):3–26.
29. Hepner A, Porter J, Hare F, et al. Serum Neurofilament Light, Glial Fibrillary Acidic Protein and Tau Are Possible Serum Biomarkers for Activity of Brain Metastases and Gliomas. World J Oncol 2019;10(4-5):169–175.
30. Chien CY, Yang Y, Gong Y, Yue Y, Chen H. Blood-Brain Barrier Opening by Individualized Closed-Loop Feedback Control of Focused Ultrasound. BME Frontiers, 2022;2022:9867230https://doi.org/10.34133/2022/9867230.
31. Vlachos F, Tung YS, Konofagou EE. Permeability assessment of the focused ultrasound-induced blood-brain barrier opening using dynamic contrast-enhanced MRI. Phys Med Biol 2010;55(18):5451–5466.
32. Lipsman N, Meng Y, Bethune AJ, et al. Blood-brain barrier opening in Alzheimer's disease using MR-guided focused ultrasound. Nat Commun 2018;9(1):2336.
33. Rezai AR, Ranjan M, D'Haese PF, et al. Noninvasive hippocampal blood-brain barrier opening in Alzheimer's disease with focused ultrasound. Proc Natl Acad Sci U S A 2020;117(17):9180–9182.
34. Anastasiadis P, Gandhi D, Guo Y, et al. Localized blood-brain barrier opening in infiltrating gliomas with MRI-guided acoustic emissions-controlled focused ultrasound. Proc Natl Acad Sci U S A 2021;118(37):e2103280118.